Available online at www.sciencedirect.com

SciVerse ScienceDirect

Ceramics International 39 (2013) 6527–6531

CERAMICS INTERNATIONAL

www.elsevier.com/locate/ceramint

# Electrical conductivity of $La_{1-x}Ca_xFeO_{3-\delta}$ solid solutions ☆

Refka Andoulsi*, Karima Horchani-Naifer, Mokhtar Férid

*Physical Chemistry Laboratory of Mineral Materials and Their Applications, National Center of Research in Material Sciences Technopole Borj Cedria, B.P. 73-8027 Soliman, Tunisia*

Received 1 December 2012; received in revised form 26 January 2013; accepted 27 January 2013
Available online 1 February 2013

**Abstract**

$La_{1-x}Ca_xFeO_{3-\delta}$ solid solutions ($x=0$, 0.1, 0.2, 0.3, 0.4, 0.5 and 0.6) were investigated. The samples were prepared by the polymerizable complex route and characterized by X-ray diffraction and complex impedance spectroscopy techniques. Results reveal the formation of a single perovskite phase for the $La_{1-x}Ca_xFeO_{3-\delta}$ ($0 \le x \le 0.5$) compositions. However, the $La_{0.4}Ca_{0.6}FeO_{3-\delta}$ sample is a mixture of many phases: perovskite, calcium ferrite and iron oxide. The unsubstituted lanthanum ferrite oxide, as well as the substituted samples, exhibits an orthorhombic symmetry. The direct current conductivity analyses reveal a typical negative temperature coefficient of the resistance behaviour for all the samples. The incorporation of calcium into the lanthanum ferrite lattice results in a significant improvement of the direct current conductivity. In fact, $La_{0.8}Ca_{0.2}FeO_{3-\delta}$ oxide shows the optimal conduction value. For all the studied compositions, a change in the activation energy is highlighted around 440 °C. This behaviour is attributed to the antiferromagnetic to paramagnetic transition of lanthanum ferrite. As for the alternating current conductivity, it obeys the Jonsher's power law. The correlated barrier hopping model is proposed to describe the transport mechanism in the studied matrix.
© 2012 Elsevier Ltd and Techna Group S.r.l. All rights reserved.

*Keywords:* A. Powders: chemical preparation; C. Impedance; D. Ferrites; D. Perovskites

## 1. Introduction

Rare earth orthoferrites $LnFeO_3$ have attracted considerable attention because of their interesting physico-chemical properties and low cost of synthesis [1]. Among these oxides, $LaFeO_3$ is one of the most studied compounds. In fact, it exhibits a high stability over a wide temperature range, a defective structure and a low thermal expansion coefficient. All these features make it useful for numerous applications such as optoelectronic devices, photocatalysts, sensor material, electrodes for solid oxide fuel cells, oxygen permeable membranes [2–6], etc.

Despite the wide range of applications, considerable effort is still devoted to the improvement of the lanthanum ferrite properties. The aim is to develop higher performances which are required for the design of novel multifunctional devices. The incorporation of divalent or trivalent cations into the lanthanum or iron sub-lattices is one of the adopted alternatives [7–11]. The idea is to induce defects to the $LaFeO_3$ crystal structure that influence the redox behaviour, the transport properties, the electronic disorder, the thermal stability and the lattice structure. Various elements such as cadmium [7], aluminium [8], lead [9], antimony [10], cobalt [11] were checked and the resulting properties were studied as a function of the chemical composition. In fact, it was shown that the substitution of iron by a transition metal ion improves the $LaFeO_3$ catalytic and electrochemical properties [12,13]. Interesting magnetic and photocatalytic activities were also reported when the lanthanum is partially replaced by a rare or alkaline earth cation [14,15].

To our knowledge, few investigations were devoted to the study of the lanthanum ferrite impedance [10]. Thus, in our previous work, an attempt was made to investigate the effect of low calcium amounts on the $LaFeO_3$ electrical properties [16]. The obtained results encouraged us to extend the range of $Ca^{2+}$ concentration and to explore its effect on the impedance behaviour. Therefore, we report in this work the study of the $La_{1-x}Ca_xFeO_{3-\delta}$ ($x=0$, 0.1, 0.2, 0.3, 0.4, 0.5 and 0.6) solid solutions. The solubility

☆ Foundation item: Project supported by the Ministry of Higher Education and Scientific Research of Tunisia.
*Corresponding author. Tel.: +216 79 325 470; fax: +216 79 325 314.
*E-mail address:* andoulsi.refka@yahoo.fr (R. Andoulsi).

0272-8842/$ - see front matter © 2012 Elsevier Ltd and Techna Group S.r.l. All rights reserved.
http://dx.doi.org/10.1016/j.ceramint.2013.01.085

limit of $Ca^{2+}$ into the $LaFeO_3$ matrix, the conductivity and the transport properties are discussed.

## 2. Material and methods

$La_{1-x}Ca_xFeO_{3-\delta}$ compositions ($0 \le x \le 0.6$) were prepared by the polymerizable complex method under the same conditions. A detailed description of the preparation was given in our previous work [17]. To implement this work, the reagents are lanthanum nitrate ($La(NO_3)_3 \cdot 6H_2O$, FLUKA, 99%), iron nitrate ($Fe(NO_3)_3 \cdot 9H_2O$, MERCK, 99%), calcium nitrate ($Ca(NO_3)_2 \cdot 4H_2O$, FLUKA, 99%), anhydrous citric acid ($C_6H_8O_7$, Renal Budapest, 99.8%) and ethylene glycol ($C_2H_6O_2$, Prolabo, 99.8%). Appropriate amounts of metal nitrates were dissolved in distilled water. Anhydrous citric acid and ethylene glycol were added to the aqueous mixture under continuous stirring. The obtained solution was heated at 130 °C yielding a glassy gel. To obtain the desired lanthanum ferrite powder, the gel was decomposed at 300 °C and calcined at 900 °C.

All the prepared compositions were characterized by an X-ray diffractometer (Siemens D500) operating with Cu kα radiation at room temperature. The International Center for Diffraction Data (ICDD) cards were used to identify the crystalline phases. In addition to the structural characterization, the lanthanum ferrite compounds were also subjected to complex impedance analysis. To perform the measurements, the synthesized powders were compacted by an hydraulic press to form pellets. Platinum electrodes were deposited on the opposite faces of the pellet. The impedance measurements were carried out in the frequency range from 5 Hz to 13 MHz between 350 and 800 °C, using a computer controlled impedance analyzer (HP 4192A).

## 3. Results and discussion

The X-ray diffraction patterns of all the prepared compositions are reported in Figs. 1 and 2. The unsubstituted sample shows well defined Bragg peaks corresponding exclusively to the perovskite lanthanum ferrite oxide (ICDD Card no. 74-2203). The same phase is obtained for the calcium substituted compositions except the 60 mol%. For this calcium content, the XRD pattern reveals, in addition to the perovskite phase, the presence of other peaks corresponding to the brownmillerite $Ca_2Fe_2O_5$ (ICDD Card no. 71-2264), iron oxide $Fe_2O_3$ (ICDD Card no. 76-1821) and calcium ferrite $CaFe_4O_6$ (ICDD Card no. 72-0891) (Fig. 2). Therefore, under the adopted preparative conditions, the lanthanum ferrite lattice can sustain at least 50 mol% of $Ca^{2+}$. From the structural side, the unsubstituted lanthanum ferrite oxide, as well as the substituted samples, crystallizes in the orthorhombic symmetry.

In addition to the XRD analyses, lanthanum ferrite compounds were also characterized by complex impedance spectroscopy. Given that the secondary phases, obtained for the $La_{0.4}Ca_{0.6}FeO_{3-\delta}$ composition, may influence the

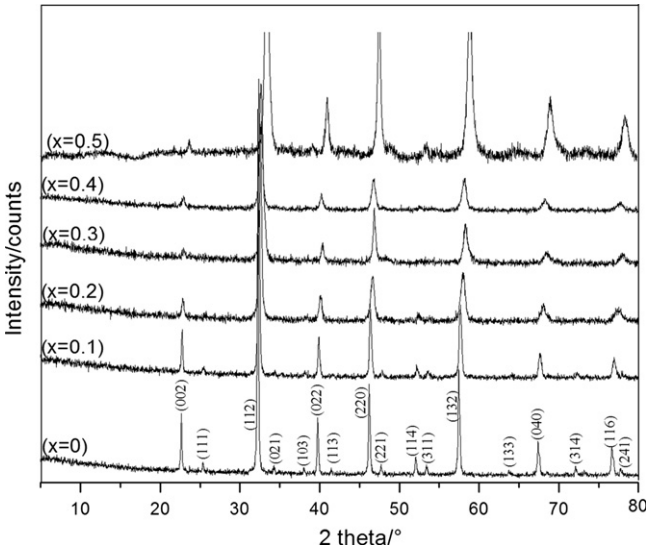


Fig. 1. XRD patterns of $La_{1-x}Ca_xFeO_{3-\delta}$ oxides ($x=0$, 0.1, 0.2, 0.3, 0.4 and 0.5).

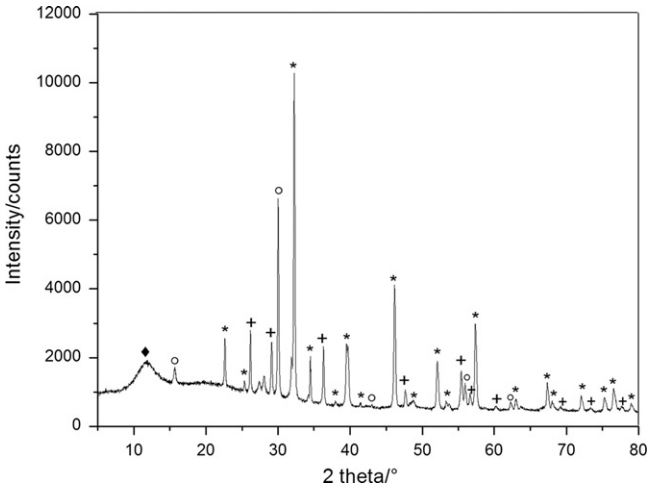


Fig. 2. XRD pattern of the $La_{0.4}Ca_{0.6}FeO_{3-\delta}$ oxide. Peak identification: (*) perovskite, (+) brownmillerite: $Ca_2Fe_2O_5$, (°) iron oxide: $Fe_2O_3$, (♦) calcium ferrite oxide: $CaFe_4O_6$.

impedance behaviour; only the conductivity of the single perovskite phases is reported below for comparison purposes.

Fig. 3 depicts the $LaFeO_3$ complex impedance spectra measured at different temperatures. These plots exhibit single semi-circular arcs. Similar trends are observed for the other lanthanum ferrite compositions. The interception of the semi-circles on the real axis towards low frequency is used to estimate the material's resistance. Consequently, the direct current conductivity ($\sigma_{dc}$) can be calculated using the following equation.

$$\sigma_{dc} = \frac{t}{dR_b} \quad (1)$$

where $R_b$ is the bulk resistance of the sample, $t$ stands for the thickness of the sample pellet and $d$ is its area.

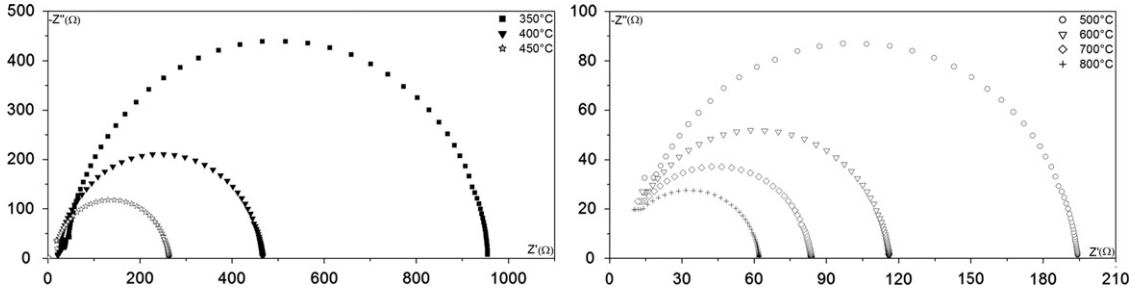


Fig. 3. Complex impedance plots of $LaFeO_3$ oxide at different temperatures.

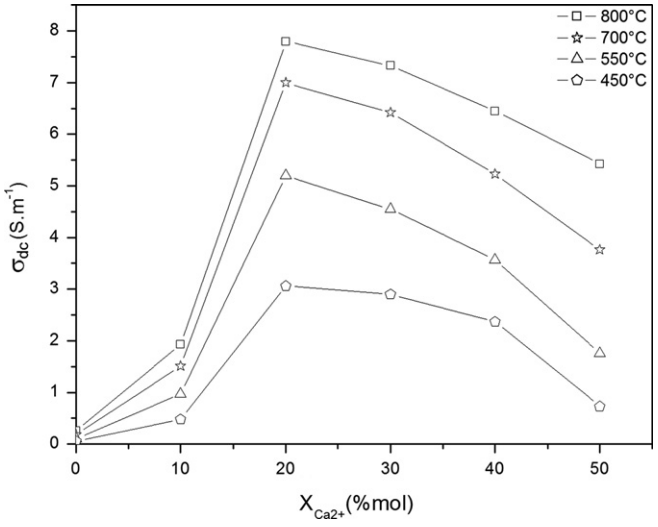


Fig. 4. Electrical conductivity variation as a function of the calcium concentration at different temperatures.

The increase in temperature shifts progressively the center of the impedance arc recorded at 350 °C towards the origin of the complex plane plots (Fig. 3). This displacement suggests an increase in the $LaFeO_3$ direct current conductivity. In fact, the highest value is obtained at 800 °C. It is about 16 times higher than the one recorded at 350 °C. Thus, the studied material exhibits a semiconductor behaviour characterized by a typical negative temperature coefficient of its resistance [18].

The evolution of the electrical conductivity versus the calcium amount was also examined. The obtained results are shown in Fig. 4. As we clearly see, the incorporation of $Ca^{2+}$ ions into the lanthanum sub-lattice increases the lanthanum ferrite electrical conductivity until a maximum value for the 20 mol% substituted compound. Indeed, at 800 °C, the $La_{0.8}Ca_{0.2}FeO_{3-\delta}$ electrical conductivity is about 30 orders of magnitude higher than that of $LaFeO_3$. The reason for this enhancement could be related to the increase in the charge carriers' concentration with $Ca^{2+}$ content. A further increase in the substituent amount leads to a decrease in the electrical conductivity. In fact, at 800 °C, the direct current conductivity ($\sigma_{dc}$) drops from 7.8 (for $La_{0.8}Ca_{0.2}FeO_{3-\delta}$) to 5.4 S m$^{-1}$ (for $La_{0.5}Ca_{0.5}FeO_{3-\delta}$) (Fig. 4). A possible explanation of this decrease is that for high $Ca^{2+}$ amounts the conduction path decreases as a result of a local distortion of the lanthanum ferrite lattice. Such distortion originates probably from the difference in the charge and ionic radii between lanthanum and calcium cations ($r_{Ca^{2+}} = 1.34$ Å, $r_{La^{3+}} = 1.36$ Å) [19].

To estimate the activation energy ($E_a$) of the conduction process, we plotted in Fig. 5 the variation of Ln ($\sigma_{dc}T$) versus the inverse of temperature for the different prepared compositions. The observed linear fit suggests that the conduction process obeys the Arrhenius law given by Eq. (2). The activation energy can be then calculated from the slope of the obtained curve. For all the studied compositions, the slope break, which is observed around 440 °C, indicates the presence of two activation energies within the studied temperature range. As listed in Table 1, $E_a$ varies from 0.43 to 0.69 eV between 350 and 440 °C. Beyond 440 °C, it decreases to 0.21–0.44 eV. For each composition, the change in $E_a$ value around 440 °C could be attributed to the second order antiferromagnetic to paramagnetic transition of lanthanum ferrite which was reported by Selbach et al. [20].

Among all the prepared compositions, $La_{0.8}Ca_{0.2}FeO_{3-\delta}$ sample exhibits the lowest activation energy and the highest conductivity. Calcium substitution may be then a way to decrease the $LaFeO_3$ resistance which is required for some applications.

$$\boldsymbol{\sigma}_{dc} = \boldsymbol{\sigma}_0 \exp\left(-\frac{E_a}{kT}\right) \quad (2)$$

where $\sigma_0$ denotes the pre-exponential factor, $T$ is the temperature and $k$ is the Boltzmann constant.

To investigate further on the electrical transport mechanism within the lanthanum ferrite matrix, we studied the variation of the alternating current conductivity ($\sigma_{ac}$) in terms of frequency. For this purpose, we chose the $LaFeO_3$ oxide as a representative example. As shown in Fig. 6, $\sigma_{ac}$ remains constant in the low frequency region. However, for high frequency values, it increases sharply. Such tendency reveals that $\sigma_{ac}$ follows the Jonsher's universal power law given by the following equation:

$$\sigma_{ac}(w) = \sigma_{dc} + Aw^s \quad (3)$$

where $w$ is the angular frequency, $A$ is the temperature pre-exponential factor and $S$ is the power law exponent determined from the slope of Ln ($\sigma_{ac}$) versus Ln ($w$) plot [21].

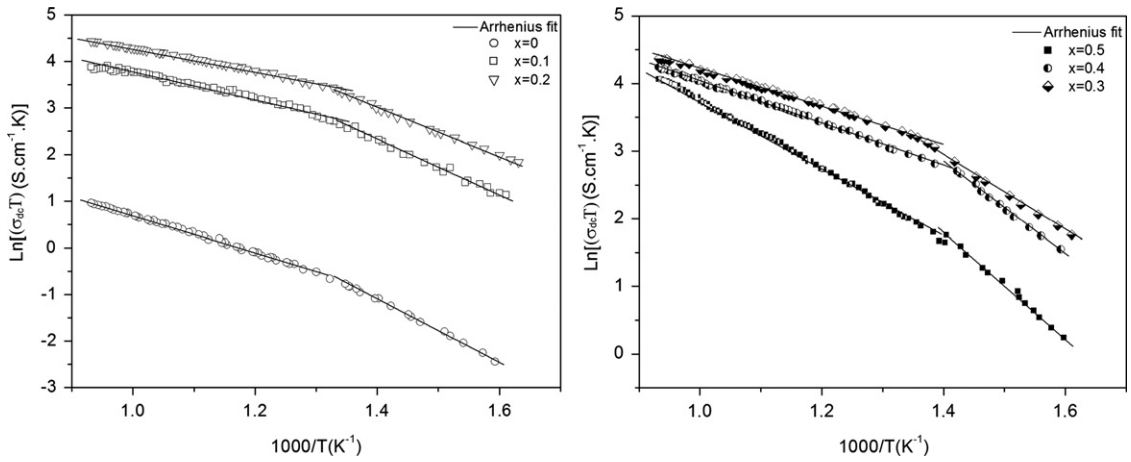


Fig. 5. Arrhenius plots of electrical conductivity for $La_{1-x}Ca_xFeO_{3-\delta}$ oxides ($x$=0, 0.1, 0.2, 0.3, 0.4 and 0.5).

Table 1
Activation energies of the conduction process for the $La_{1-x}Ca_xFeO_{3-\delta}$ perovskites ($x$=0, 0.1, 0.2, 0.3, 0.4 and 0.5).

| $La_{1-x}Ca_xFeO_{3-\delta}$ | $E_a$ (eV) | |
|---|---|---|
| $x$ | 350–440 °C | 440–800 °C |
| 0 | 0.64 | 0.36 |
| 0.1 | 0.46 | 0.26 |
| 0.2 | 0.43 | 0.21 |
| 0.3 | 0.56 | 0.23 |
| 0.4 | 0.6 | 0.25 |
| 0.5 | 0.69 | 0.44 |

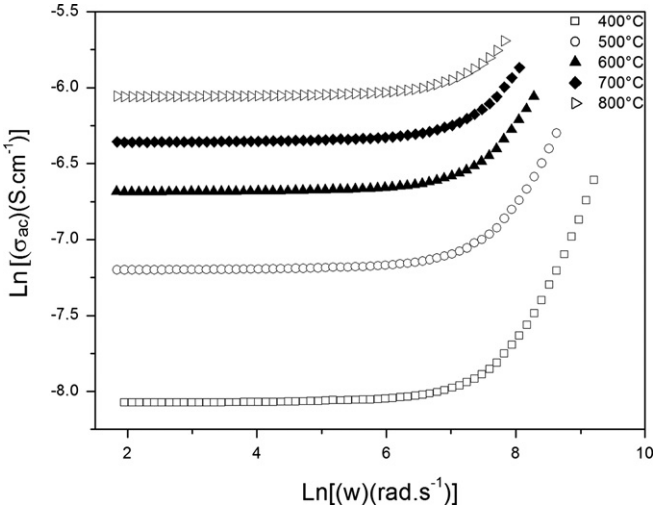


Fig. 6. Variation of $LaFeO_3$ alternating current conductivity ($\sigma_{ac}$) versus the frequency at different temperatures.

According to the Jonsher's law, two models can be used to describe the dependence of the alternating current conductivity on high frequencies: the quantum mechanical tunnelling model [22] for which the frequency exponent $S$ is temperature independent and the correlated barrier hopping model [23] that predicts a decrease in $S$ value with temperature increase. Based on our experimental results, $S$ is a function of temperature. In fact, it decreases from 0.86 to 0.36 when temperature passes from 400 to 800 °C (Table 2). The correlated barrier hopping model is, therefore, adequate to describe the conduction mechanism within the lanthanum ferrite lattice. Accordingly, the transport of charge carriers could be summarized as follows: at low frequency side, the transport takes place via infinite percolation path. However, for high frequencies, the transport is due to the hopping of charge carriers in finite clusters [23].

Table 2
Calculated values of $S$, $\sigma_{ac}$ and $W_m$ at different temperatures for $LaFeO_3$.

| Temperature (°C) | $S$ | $\sigma_{ac}$ (S m$^{-1}$) | $W_m$ (eV) |
|---|---|---|---|
| 400 | 0.86 | 0.05 | 2.48 |
| 500 | 0.71 | 0.12 | 1.38 |
| 600 | 0.61 | 0.2 | 1.15 |
| 700 | 0.46 | 0.28 | 0.93 |
| 800 | 0.36 | 0.32 | 0.86 |

Since the alternating current conductivity depends on the binding energy $W_m$ (energy required to remove a charge carrier and to transfer it from one site to another) [24], we calculated $W_m$ using the following equation. Table 2 lists the obtained values for the $LaFeO_3$ oxide. The binding energy tends to decrease with temperature. Such behaviour explains the increase in the alternating current conductivity when the temperature increases.

$$W_m = \frac{6Tk}{1-S} \quad (4)$$

where $k$ is the Boltzmann constant and $T$ is the temperature [23].

## 4. Conclusion

The present work deals with the preparation and characterization of the $La_{1-x}Ca_xFeO_{3-\delta}$ ($x$=0–0.6) solid solutions. To

synthesize the desired compositions, the polymerizable complex method is efficient and reproducible. Based on the XRD results, we showed that the $La_{1-x}Ca_xFeO_{3-\delta}$ ($x=0$–0.5) compounds have a single orthorhombic perovskite structure. However, the $La_{0.4}Ca_{0.6}FeO_{3-\delta}$ composition is a mixture of many phases: perovskite, iron oxide and calcium ferrite. The conduction properties of the single phases were investigated by means of complex impedance technique. The obtained results reveal an increase in the direct current conductivity with the calcium concentration until a maximum value (7.8 $S\,m^{-1}$ at 800 °C) for the $La_{0.8}Ca_{0.2}FeO_{3-\delta}$ oxide. For each composition, the activation energy decreases beyond 440 °C. Such behaviour is attributed to the second order magnetic transition of lanthanum ferrite. The conduction process is thermally activated and the correlated barrier hopping model is suitable for the description of the transport properties in the lanthanum ferrite matrix.

## Acknowledgement

This work is supported by the Ministry of Higher Education and Scientific Research in Tunisia.

## References

[1] Z.L. Wang, Z.C. Kang, in: Functional and Smart Materials, Second ed., Plenum Press, New York, 1998.
[2] E.A. Tugova, V.F. Popova, I.A. Zvereva, V.V. Gusarov, Phase diagram of the $LaFeO_3$–$LaSrFeO_4$ system, Glass Phys. Chem. 32 (2006) 674–676.
[3] S. Petrovic, A. Terlecki, L. Karanovic, P. Kirilov-Stefanov, M. Zduji, V. Dondur, D. Paneva, I. Mitov, V. Rakic, $LaMO_3$ (M=Mg, Ti, Fe) perovskite type oxides: preparation, characterization and catalytic properties in methane deep oxidation, Appl. Catal. B 79 (2008) 186–198.
[4] S.N. Tijare, M.V. Joshi, P.S. Padole, P.A. Mangrulkar, S. Rayalu, N.K. Labhsetwar, Photocatalytic hydrogen generation through water splitting on nano-crystalline $LaFeO_3$ perovskite, Int. J. Hydrogen Energy 37 (2012) 10451–10456.
[5] Z. Wei, Y. Xu, H. Liu, C. Hu, Preparation and catalytic activities of $LaFeO_3$ and $Fe_2O_3$ for HMX thermal decomposition, J. Hazard. Mater. 165 (2009) 1056–1061.
[6] J. Faye, A. Bayleta, M. Trentesauxb, S. Royera, F. Dumeignil, D. Duprez, S. Valange, Influence of lanthanum stoichiometry in $La_{1-x}FeO_{3-\delta}$ perovskites on their structure and catalytic performance in $CH_4$ total oxidation, J. Appl. Catal. B 126 (2012) 134–143.
[7] M. Bellakki, V. Manivannan, J. Das, Synthesis, structural and magnetic properties of $La_{1-x}Cd_xFeO_3$ ($0.0 \le x \le 0.3$) orthoferrites, Mater. Res. Bull. 44 (2009) 1522–1527.
[8] P. Ciambelli, S. Cimino, G. Lasorella, L. Lisi, S. De Rossi, M. Faticanti, G. Minelli, P. Porta, CO oxidation and methane combustion on $LaAl_{1-x}Fe_xO_3$ perovskite solid solutions, Appl. Catal. B 37 (2002) 231–241.
[9] L. Zhang, J. Hu, P. Song, H. Qin, M. Jiang, Electrical properties and ethanol-sensing characteristics of perovskite $La_{1-x}Pb_xFeO_3$,, Sensors Actuators B 114 (2006) 836–840.
[10] L. Berchmans, R. Sindhu, S. Angappan, C.O. Augustin, Effect of antimony substitution on structural and electrical properties of $LaFeO_3$, J. Mater. Process. Technol. 207 (2008) 301–306.
[11] M.R. Goldwasser, M.E. Rivas, M.L. Lugo, E. Pietri, J. Perez-Zurita, M.L. Cubeiro, A. Griboval, G. Leclercq, Combined methane reforming in presence of $CO_2$ and $O_2$ over $LaFe_{1-x}Co_xO_3$ mixed-oxide perovskites as catalysts precursors, Catal. Today 107 (2005) 106–113.
[12] K. Kammer, L. Mikkelsen, J. Bilde, Electrical and electro-chemical characterization of $La_{0.99}Fe_{1-x}Ni_xO_{3-\delta}$ perovskites, J. Solid State Electrochem. 10 (2006) 934–940.
[13] S. Hosseini, M. Sadeghi, A. Alemi, A. Niaei, D. Salari, L. Kafi, Synthesis, characterization, and performance of $LaZn_xFe_{1-x}O_3$ perovskite nanocatalysts for toluene combustion, Chin. J. Catal. 31 (2010) 747–750.
[14] F. Li, Y. Liu, R. Liu, Z. Sun, D. Zhao, C. Kou, Preparation of Ca-doped $LaFeO_3$ nanopowders in a reverse microemulsion and their visible light photocatalytic activity, Mater. Lett. 64 (2010) 223–225.
[15] A. Mahmood, M.F. Warsi, M.N. Ashiq, M. Ishaq, Substitution of La and Fe with Dy and Mn in multiferroic $La_{1-x}Dy_xFe_{1-y}Mn_yO_3$ nanocrystallites, J. Magn. Magn. Mater. 327 (2013) 64–70.
[16] R. Andoulsi, K. Horchani-Naifer, M. Férid, Structural and electrical properties of calcium substituted lanthanum ferrite powders, Powder Technol. 230 (2012) 183–187.
[17] R. Andoulsi, K. Naifer, M. Ferid, Preparation of lanthanum ferrite powder at low temperature, Ceramica 58 (2012) 126–130.
[18] M. Baazaoui, S. Zemni, M. Boudard, H. Rahmouni, M. Oumezzine, A. Selmi, Conduction mechanism in $La_{0.67}Ba_{0.33}Mn_{1-x}Fe_xO_3$ ($x=0$–0.2) perovskites, Physica B 405 (2010) 1470–1474.
[19] M.A. Ahmed, S.I. El-Dek, Extraordinary role of $Ca^{2+}$ ions on the magnetization of $LaFeO_3$ orthoferrite, Mater. Sci. Eng. B 128 (2006) 30–33.
[20] S.M. Selbach, J.R. Tolchard, A. Fossdal, T. Grande, Non-linear thermal evolution of the crystal structure and phase transitions of $LaFeO_3$ investigated by high temperature X-ray diffraction, J. Solid State Chem. 196 (2012) 249–254.
[21] A.K. Jonsher, The universal dielectric response, Nature 267 (1977) 673–679.
[22] I.G. Austin, N.F. Mott, Polarons in crystalline and non-crystalline materials, Adv. Phys. 18 (1969) 41.
[23] S. Mollah, K. Som, K. Bose, B.K. Chaudhuri, AC conductivity in $Bi_4Sr_3Ca_3Cu_yO_x$ ($y=0$–5) and $Bi_4Sr_3Ca_{3-z}Li_zCu_4O_x$ ($z=0.1$–1.0) semiconducting oxide glasses, J. Appl. Phys. 74 (1993) 931.
[24] S.R. Elliott, AC conduction in amorphous chalcogenide and pnictide semiconductors, Adv. Phys. 36 (1987) 135–218.